Radiative decay of J/ψ into $\eta(1430)$ and nearby states

J.-E. Augustin, G. Cosme, F. Couchot, F. Fulda, G. Grosdidier, B. Jean-Marie, V. Lepeltier, F. Mane, and G. Szklarz
Laboratoire de l'Accélérateur Linéaire, Université de Paris-Sud, F-91405 Orsay, France

J. Jousset, Z. Ajaltouni, A. Falvard, B. Michel, and J. C. Montret
Laboratoire de Physique Corpusculaire, Université de Clermont II, Boîte Postale 45, F-63170 Aubière, France

R. Baldini and A. Calcaterra
Laboratori Nazionali di Frascati dell'Istituto Nazionale de Fisica Nucleare, Cassella Postale 13, I-00044 Frascati, Italy

D. Bisello, G. Busetto, A. Castro, L. Pescara, P. Sartori, and L. Stanco
Dipartimento di Fisica dell'Università di Padova, e Istituto Nazionale de Fisica Nucleare, Sezione di Padova, I-35131 Padua, Italy

(DM2 Collaboration)
(Received 2 January 1990)

Radiative decays of J/ψ into $K^+K^-\pi^0$, $K_S^0K^\pm\pi^\mp$, $\eta\pi^+\pi^-$, and $\rho\gamma$ have been studied in the $\eta(1430)$ mass range from the $8.6\times10^6 J/\psi$'s produced in the DM2 experiment at the Orsay e^+e^- storage ring (DCI). The $\eta(1430)$ is observed in both $K_S^0K^\pm\pi^\mp$ and $K^+K^-\pi^0$ channels. A three-body decay-angular analysis of the whole signal supports a $J^P=0^-$ assignment. A substantial $KK^*(892)$ dynamics is present whereas the significance of the $a_0(980)\pi$ contribution cannot be evaluated. The $\eta(1430)$ is not observed in the $\eta\pi\pi$ channel which shows a peak in the $f_1(1285)/\eta(1275)$ mass range and a new state at 1398 MeV/c^2, $\simeq$50 MeV/c^2 wide. An $a_0(980)\pi$ intermediate-state contribution is present at least in the latter state. Finally, the low-statistics $\rho\gamma$ final state gives no evidence of $\eta(1430)$ production.

I. INTRODUCTION

As pointed out long ago[1] the J/ψ radiative decays into one photon and two gluons are well suited to look for exotic states with large gluon content such as glueballs. The nature and the decays of one of these candidates, the $\eta(1430)$ (previously ι), are a long-standing problem. First found in the J/ψ radiative decays[2,3] into $K\bar{K}\pi$ the $\eta(1430)$ is suspected to have a large glue content due to its large production rate. Moreover the $\eta(1430)$ owns an isoscalar and pseudoscalar assignment whereas the isoscalar component of the 0^{-+} nonet corresponding to the first $q\bar{q}$ radial excitation is already filled up by the $\eta(1275)$.[4] Nevertheless earlier QCD predictions[5] foresee a pseudoscalar activity in the $\eta(1430)$ mass range.

On the other hand, at about the same mass, experiments on hadroproduction have also observed states[6] whose spin-parity are still controversial. If $p\bar{p}$ at rest produces $\eta(1430)$, other experiments favor a $J^P=1^+$ assignment which would identify it with the $f_1(1420)$. Many authors suggest a composite nature of the $\eta(1430)$ signal in radiative J/ψ decays. In particular[7] contributions of at least an axial-vector and a pseudoscalar state at roughly the same mass should be present. Recent measurements based on different hadroproduction mechanisms give evidence of both axial-vector and pseudoscalar production in this mass range.[8]

Furthermore the experiments show also contradictory results concerning the dynamics of the $K\bar{K}\pi$ system in the $\eta(1430)$ mass region. The $KK^*(892)$ intermediate state seems favored in hadronic productions whereas J/ψ radiative decays in a previous experiment[3] gave an upper limit for the ratio $B(KK^*)/B(KK^*+a_0\pi)<0.25$ and the low-$K\bar{K}$-mass enhancement was assigned to the $a_0(980)\pi$ intermediate state. The $a_0(980)\pi$ dominance should require the $\eta(1430)$ observation into $\eta\pi\pi$ but clear evidence of such a decay has not been found yet, although some pseudoscalar activity has been reported in this mass range.[9]

Finally the $\eta(1430)$ radiative decay into a vector meson could provide a good glueball signature. The $\eta(1430)$ radiative width[10,11] should be between 1–4 MeV/c^2 for a glueball and 0.1–1 MeV/c^2 for a purely hadronic state. However mixture between the two sectors can totally change this picture.

This paper presents improved measurements by the DM2 experiment on the search for the $\eta(1430)$ production in the $J/\psi\to\gamma K^+K^-\pi^0$, $J/\psi\to\gamma K_S^0K^\pm\pi^\mp$, $J/\psi\to\gamma\eta\pi^+\pi^-$, and $J/\psi\to\gamma\rho\gamma$ channels. The results are obtained from 8.6×10^6 J/ψ's produced with the e^+e^- Orsay storage ring DCI. After a short description of the DM2 apparatus (Sec. II), the analysis of the $K_S^0K^\pm\pi^\mp$ and $K^+K^-\pi^0$ final states are reported in Sec. III. The results for other decay modes, $\gamma\eta\pi\pi$ and $\gamma\rho\gamma$, are presented in Secs. IV and V, respectively.

A full wave analysis of $J/\psi\to\gamma K\bar{K}\pi$ and $J/\psi-\gamma\eta\pi^+\pi^-$ and the interpretation of the obtained results will be presented in a forthcoming paper.

II. EXPERIMENTAL SETUP

The DM2 detector[12] is a large-solid-angle magnetic spectrometer. A 2-m-diam and 3-m-long solenoid with a $1X_0$ aluminum coil produces a 0.5-T magnetic field. Inside two proportional and 13 drift chambers allow the detection of charged particles over a solid angle of $0.87\times 4\pi$ sr, with a momentum resolution of 3.5% at 1 GeV/c. A set of 36 2-cm-thick scintillators provides a time-of-flight measurement with a total resolution of 540 ps, including 440 ps from the beam spread, allowing a 3σ π/K separation up to 450 MeV/c.

The photon-detector barrel ($6X_0$), divided into octants, is outside the coil. It mainly consists of 14 planes of streamer tubes with a delay line sandwiched with lead and scintillator planes. The barrel covers a solid angle of $0.7\times 4\pi$ sr, with a detection efficiency greater than 96% above 110 MeV and a spatial resolution for the photon direction of 10 mrad in azimuth and 7 mrad in polar angle. The detector has tracking capabilities and matching is performed with the tracks in the drift chamber. Two end-cap detectors of $5X_0$ each are inside the magnetic field, covering 12% of the solid angle. Because of the limited angular resolution this detector is used only as veto to define the requested topologies.

III. $K\bar{K}\pi$ ANALYSIS

A. $K_S^0K^{\pm}\pi^{\mp}$ final state

The analysis of this channel[13] corresponds to events with four charged tracks of zero total charge and one photon in the barrel detector. For each event, all possible mass assignments for the tracks are successively considered. Then the following cuts are made: (i) The $\pi^+\pi^-$ mass of the supposed K_S^0 must lie within 35 MeV/c^2 around the K_S^0 mass; (ii) the total reconstructed energy has to match the J/ψ mass within 110 MeV/c^2; (iii) the photon coplanarity is ensured by requiring $p_T^2=4p_{\rm miss}^2\sin^2\theta/2<4000$ (MeV/c)^2, where $p_{\rm miss}$ is the missing momentum to the charged tracks and θ the angle between the photon and the missing momentum. Furthermore the mass assignments are checked with the available time-of-flight (TOF) information and the global probability of the considered combination has to be $P(\chi^2)>2\%$. However no TOF measurement is required to retain the events which are then three- and four-constraint (3C and 4C) fit (K_S^0 mass imposed) and rejected if $\chi^2_{3C}\geq 6$ and $\chi^2_{4C}\geq 11$. In addition, to improve the rejection of the background from the $J/\psi\to\gamma\pi^+\pi^-\pi^+\pi^-$ and $\pi^+\pi^-\pi^+\pi^-\pi^0$ decays, a 3C fit is made assuming all the particles to be pions and the events with $\chi^2_{4\pi}\leq(\chi^2_{KK\pi}+4)$ are discarded. All the cuts have been set by Monte Carlo studies and extensively checked on the experimental events. In 85% of the cases only one combination passes through all the cuts. When more than one combination survives all the cuts, the one with the best fit is retained.

The scatter plots of $K_S^0K\pi$ mass versus the $K_S^0K^{\pm}$ and $(K_S^0\pi^{\pm}+K^{\pm}\pi^{\mp})$ masses show a cluster of events in the $1300<m_{K_S^0K\pi}<1600$ MeV/c^2 mass region [Figs. 1(a) and 1(b)].

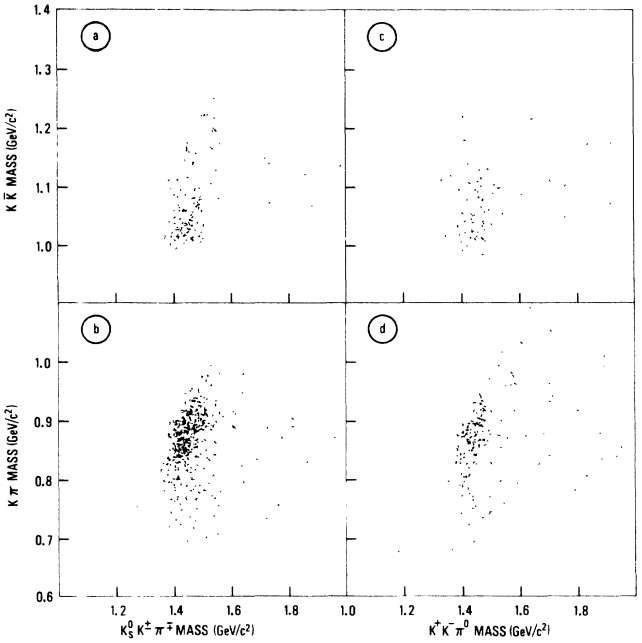

FIG. 1. (a) $K_S^0K^{\pm}\pi^{\mp}$ mass vs $K_S^0K^{\pm}$ and (b) $(K_S^0,K^{\pm})\pi^{\mp}$ mass-scatter plots for $J/\psi\to\gamma K_S^0K^{\pm}\pi^{\mp}$ events. (c) $K^+K^-\pi^0$ mass vs K^+K^- and (d) $K^{\pm}\pi^{\mp}$ mass-scatter plots for $J/\psi\to\gamma K^+K^-m^0$ events.

The $K_S^0K^{\pm}\pi^{\mp}$ invariant-mass spectrum shown in Fig. 2(a) is clearly asymmetric and difficult to fit into a single conventional Breit-Wigner form; it rather suggests the presence of threshold effects and/or more than one state. Assuming a single resonance[14] the best fit has been obtained using a Breit-Wigner curve folded with KK^* phase space added to a polynomial background, and leads to the following parameters ($\chi^2=34/35$ DF):

$$m_{\eta(1430)}=1445\pm 8\ \text{MeV}/c^2\ ,$$

$$\Gamma_{\eta(1430)}=105\pm 10\ \text{MeV}/c^2\ .$$

On the contrary the standard unfolded fit gives the following results ($\chi^2=48/35$ DF):

$$m_{\eta(1430)}=1456\pm 8\ \text{MeV}/c^2\ ,$$

$$\Gamma_{\eta(1430)}=88\pm 9\ \text{MeV}/c^2\ .$$

By varying the background shapes, the two classes of fit do not undergo noticeable changes except for the peak position. The reported $\eta(1430)$ mass errors account for this effect. The branching ratio has been calculated from the 693 ± 30 events present in the 1350–1550-MeV/c^2 mass range after background subtraction. The efficiency varies from 11% for an isotropic decay of the $\eta(1430)$ to 13% when $KK^*(892)$ or $a_0(980)\pi$ dynamics are as-

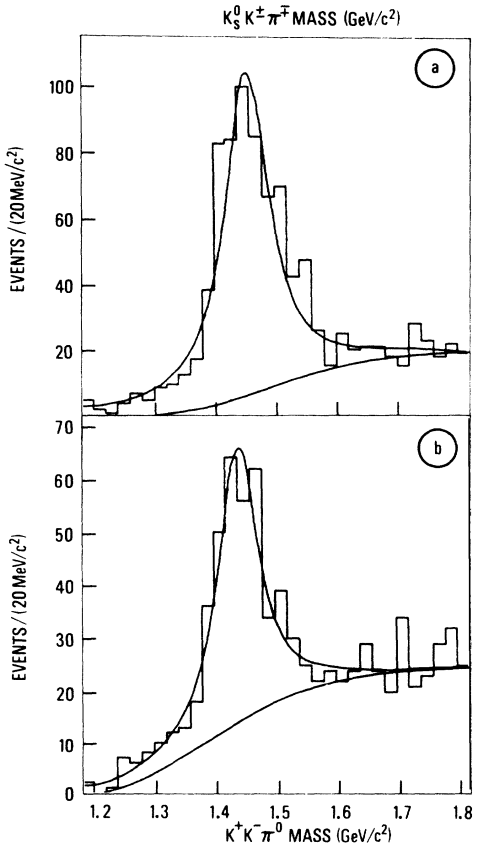

FIG. 2. (a) Fit of the $\eta(1430)$ signal for $J/\psi \to \gamma K_S^0 K^\pm \pi^\mp$ and for (b) $J/\psi \to \gamma K^+ K^- \pi^0$ events. The curves refer to the unfolded Breit-Wigner fits.

sumed. Using an average value of (12.0±0.5)% the following value is obtained:

$$B(J/\psi \to \gamma\eta(1430))B(\eta(1430) \to K_S^0 K\pi) = (1.20 \pm 0.05 \pm 0.20) \times 10^{-3} .$$

The quoted systematic error comes from the uncertainty on normalization[15] quadratically added to the uncertainties on the fit procedure and background estimation.

B. $K^+K^-\pi^0$ final state

Events with two charged tracks and three photons in the barrel detector are selected. The photon energies are calculated by imposing energy-momentum conservation, assuming kaon masses for the charged tracks. The events are two-constraint (2C) fit to the $J/\psi \to \gamma K^+ K^- \pi^0$ hypothesis, the invariant mass of the two lower-energy photons being constrained to the π^0 mass. Events with $\chi^2 > 3$ are discarded. Fake π^0 contamination coming from very unbalanced photons is removed by a cut (< 0.98) on the cosine of the angle θ^* between the γ direction and the boost direction of the π^0 in its rest frame. Finally at least one of the two charged tracks must have a TOF measurement compatible to a kaon hypothesis within 2.5σ.

The scatter plots of Figs. 1(c) and 1(d) show a clear $\eta(1430)$ signal in the $K^+K^-\pi^0$ invariant-mass distribution. A fit to a Breit-Wigner curve folded with KK^* phase space added to a polynomial background ($\chi^2 = 21/35$ DF) gives the parameters

$$m_{\eta(1430)} = 1433 \pm 8 \text{ MeV}/c^2 ,$$

$$\Gamma_{\eta(1430)} = 93 \pm 14 \text{ MeV}/c^2 ,$$

whereas from the unfolded fit ($\chi^2 = 23/35$ DF) we obtain

$$m_{\eta(1430)} = 1430 \pm 8 \text{ MeV}/c^2 ,$$

$$\Gamma_{\eta(1430)} = 78 \pm 15 \text{ MeV}/c^2 .$$

The differences with the results of the $K_S^0 K\pi$ mode are mainly due to the evaluation of the background, which is different in the two channels, and are compatible with the fit systematics. From 296±20 observed events and an average efficiency of (5.0±0.3)%, calculated as above, the branching ratio is inferred:

$$B(J/\psi \to \gamma\eta(1430))B(\eta(1430) \to K^+K^-\pi^0) = (0.68 \pm 0.05 \pm 0.11) \times 10^{-3} .$$

This result is consistent with the value obtained in the

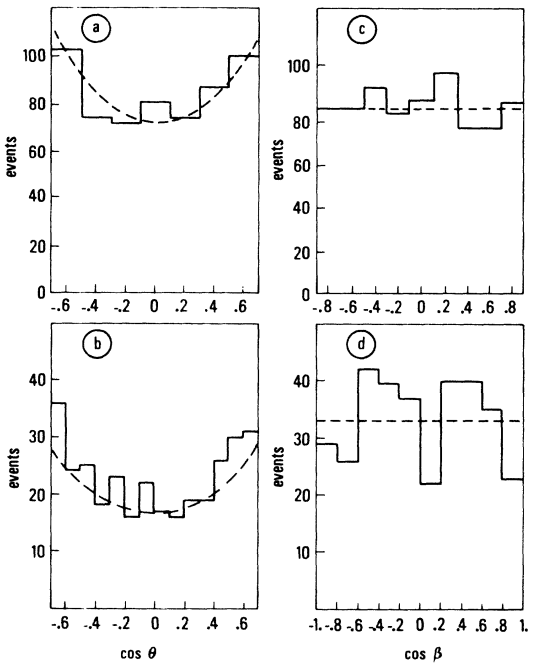

FIG. 3. (a) and (c) distribution of $\cos\theta$ and $\cos\beta$ in the mass range $1360 < m_{K\bar{K}\pi} < 1560$ MeV/c^2 for $J/\psi \to \gamma K_S^0 K^\pm \pi^\mp$ events and (b) and (d) for $J/\psi \to \gamma K^+ K^- \pi^0$ events.

TABLE I. Maximum-likelihood-fit results for the $J/\psi \to K\bar{K}\pi$ angular analysis.

	$\eta_{(1430)} \to K^+K^-\pi^0$	$\eta_{(1430)} \to K_S^0 K^{\pm}\pi^{\mp}$	$\eta_{(1430)} \to K\bar{K}\pi$
$J^P=0^-$	$\ln(L)=6.61$	$\ln(L)=1.51$	$\ln(L)=8.10$
$J^P=1^+$	$\ln(L)=-2.60$	$\ln(L)=-11.90$	$\ln(L)=-16.9$
	$x=-0.71^{+0.09}_{-0.10}$	$x=-1.05^{+0.11}_{-0.13}$	$x=-0.90^{+0.07}_{-0.08}$
$J^P=1^-$	$\ln(L)=-16.9$	$\ln(L)=-20.0$	$\ln(L)=-37.4$
	$x=-1.28^{+0.13}_{-0.11}$	$x=-1.14^{+0.08}_{-0.07}$	$x=-1.19^{+0.06}_{-0.07}$

$K_S^0 K^{\pm}\pi^{\mp}$ channel for an isoscalar state

$$\frac{2B(\eta(1430)\to K^+K^-\pi^0)}{B(\eta(1430)\to K_S^0 K^{\pm}\pi^{\mp})}=1.13\pm0.13 .$$

Therefore the branching ratio is set:

$$B(J/\psi\to\gamma\eta(1430))B(\eta(1430)\to K\bar{K}\pi) =(3.80\pm0.30\pm0.60)\times10^{-3} .$$

C. Spin-parity analysis

The spin-parity analysis of the $\eta(1430)$ has been made by using the three-body decay formalism of Berman and Jacob[16] where three angles are used: θ, the angle between the beam (z axis) and the $\eta(1430)$ direction, and β and ϕ, polar and azimuthal angles of the normal to the $\eta(1430)$ decay plane in the helicity frame. The results with this technique are almost independent of the decay process of the $\eta(1430)$, in particular of intermediate states.

The three spin-parity hypothesis 0^-, 1^+, and 1^- have been tested on the events with a $K\bar{K}\pi$ mass in the 1320–1540-MeV/c^2 range. Each hypothesis carries a definite angular distribution:

$$0^-:\ \frac{dN}{d\Omega}=1+\cos^2\theta$$

($\cos\beta$ and $\cos\phi$ distributions being uniform),

$$1^+:\ \frac{dN}{d\Omega}=(1+\cos^2\theta)\sin^2\beta+\frac{x}{2}\sin2\theta\sin2\beta\cos\phi +x^2\sin^2\theta(1+\cos^2\beta) ,$$

$$1^-:\ \frac{dN}{d\Omega}=(1+\cos^2\theta)\cos^2\beta-\frac{x}{2}\sin2\theta\sin2\beta\cos\phi +x^2\sin^2\theta\sin^2\beta ,$$

where x is the helicity-1 to helicity-0 amplitude ratio.

The experimental $\cos\theta$ and $\cos\beta$ distributions, corrected by the acceptance (Fig. 3), are compatible with a $J^P=0^-$ hypothesis. Moreover the three hypotheses are compared by using a maximum-likelihood procedure:

$$\ln(L_J)=\sum_{\text{events}}\ln\left[\frac{dN}{d\Omega}\right]_J-N_{\text{events}}\ln\sum_{i=0}^{i=2}N_{Ji}x^i ,$$

where the N_{Ji} parameters account for the apparatus acceptance in the given hypothesis and are obtained from large samples of Monte Carlo simulation events.

Table I summarizes the results: Assuming the observed structure contains only one resonance, the $J^P=0^-$ assignment is heavily favored. This result agrees with a previous small-statistics measurement.[3]

D. Dynamics of the $K\bar{K}\pi$ final state

The $K^{\pm}\pi^{\mp}+K_S^0\pi^{\mp}$ and $K^{\pm}\pi^0$ mass distributions in the 1360–1560-MeV/c^2 range [Figs. 4(a) and 4(b)] show the $k^*(892)$ signal, respectively, at 883 ± 5 MeV/c^2 and 874 ± 4 MeV/c^2. The small mass shifts from the $K^*(892)$

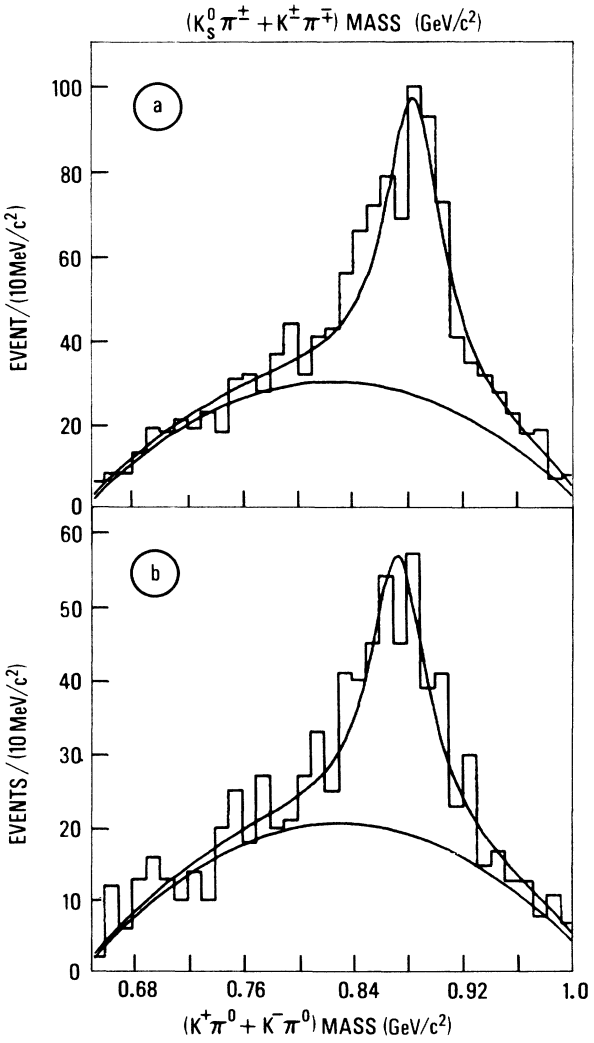

FIG. 4. (a) $K_S^0\pi^{\pm}+K^{\pm}\pi^{\mp}$ mass distribution for $J/\psi\to\gamma K_S^0 K^{\pm}\pi^{\mp}$ events and (b) $K^{\pm}\pi^{\mp}$ mass distribution for $J/\psi\to\gamma K^+K^-\pi^0$ events.

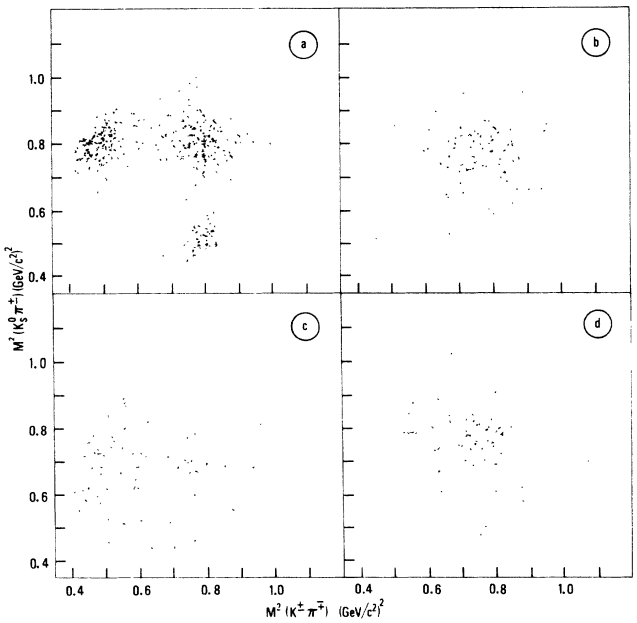

FIG. 5. (a) $K\pi$ Dalitz plot for Monte Carlo $J/\psi\to K^0_S K\pi$ events in the KK^*, (b) $a_0\pi$, (c) three-body phase space, (d) hypotheses and the experimental distribution.

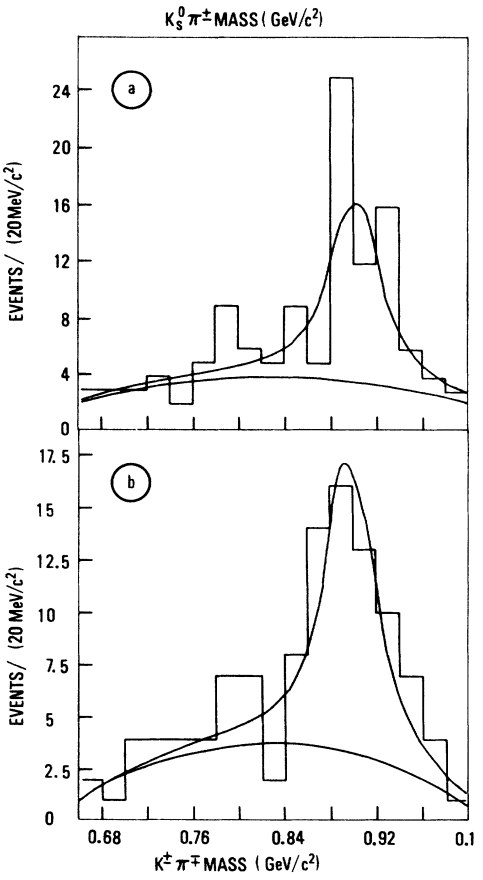

FIG. 6. Fit of the $K^*(892)$ signal for $J/\psi\to\gamma K^0_S K^\pm\pi^\mp$ events: (a) $K^*(892)\to K^0_S\pi^\mp$ and (b) $K^*(892)\to K^\pm\pi^\mp$.

mass are compatible with the fit systematics coming from phase-space effects. In order to estimate the $KK^*(892)$ contribution the Dalitz plot of both $K^0_S K^\pm\pi^\mp$ and $K^+K^-\pi^0$ are compared to $a_0(980)\pi$, $KK^*(892)$, and three-body $K\bar{K}\pi$ phase space in the $J^P=0^-$ $\eta(1430)$ spin-parity hypothesis (Fig. 5).

The $K^*(892)$ candidates are selected by requiring the other $K\pi$ charge combination to lie in the Dalitz-plot area defined by the cut $(0.4\times10^6\le m^2_{K\pi}\le0.6\times10^6$ MeV$^2/c^4$) so largely excluding the $a_0(980)\pi$ contribution which is mainly located in the Dalitz-plot region where the two $K^*(892)$ bands overlap. The same procedure is applied to each $K\pi$ charge combination. Figures 6(a), 6(b), and 7 show the $K^*(892)$ signal for $K^0_S K^\pm\pi^\mp$ and $K^+K^-\pi^0$ channels after this cut. The fit to a Breit-Wigner function plus a quadratic background gives for the ratio

$$\frac{B(\eta(1430)\to KK^*(892))}{B(\eta(1430)\to K\bar{K}\pi)}$$

0.33 ± 0.08 and 0.35 ± 0.66 for $K^+K^-\pi^0$ and $K^0_S K^\pm\pi^\mp$ modes, respectively.

The background coming from the other dynamical assumptions is calculated by applying the same method on phase space $K\bar{K}\pi$ and $a_0(980)\pi$ Monte Carlo events. The corresponding contaminations are $(3\pm1)\%$ and $(19\pm3)\%$, respectively.

In addition the $K^0_S K^\pm$ and K^+K^- mass spectra show [Figs. 8(a) and 8(b)] a large population at $m_{K\bar{K}}<1100$ MeV/c^2. This has been interpreted[3] as indication of an $a_0(980)\pi$ dominance in the $K\bar{K}\pi$ final state. To evaluate this possible $a_0(980)\pi$ dynamics, the $K\bar{K}$ spectrum is fit to a Flatté parametrization[17] plus a three-body $k\bar{K}\pi$ phase-space distribution, thus ignoring the

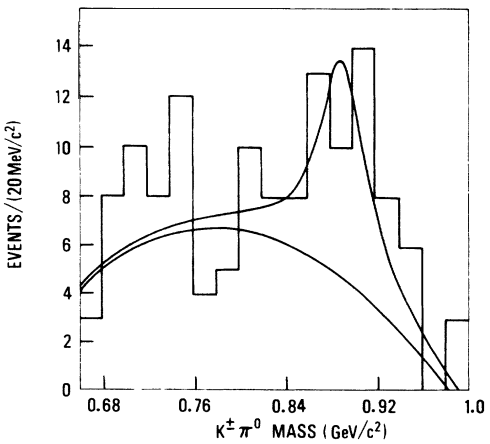

FIG. 7. Fit of the $K^{*\pm}(892)$ signal for $J/\psi\to\gamma K^+K^-\pi^0$ events.

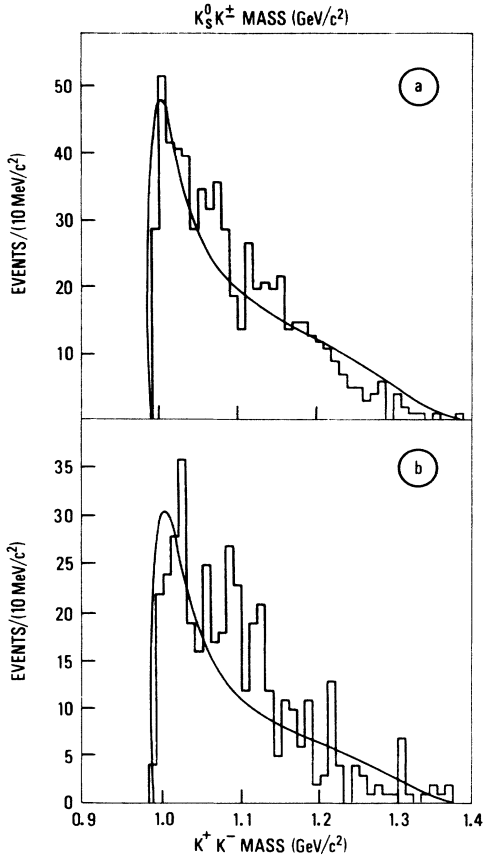

FIG. 8. $K\bar{K}$ mass distribution when $1.36 > m_{K\bar{K}\pi} > 1.56$ GeV/c^2 (a) for $J/\psi \to \gamma K^0_S K^\pm \pi^\mp$ events and (b) for $J/\psi \to \gamma K^+ K^- \pi^0$ events.

$KK^*(892)$ intermediate state. This hypothesis leads to the

$$\frac{B(\eta(1430) \to a_0(980)\pi)}{B(\eta(1430) \to K\bar{K}\pi)} = 0.50 \pm 0.25 \ .$$

However a low-$K\bar{K}$-mass accumulation is also observed in $KK^*(892)$ Monte Carlo events. The same analysis performed on such events shows that $(30 \pm 10)\%$ of this channel simulates the experimental low-$K\bar{K}$-mass behavior.

In conclusion, if any dynamics proceeds through a $J^P = 0^-$ state, this analysis gives evidence of an important $KK^*(892)$ contribution. The shape of the low-$K\bar{K}$-mass distribution is compatible with a possible, even large, $a_0(980)\pi$ dynamics but no clear evidence of this intermediate state is found within this analysis.

IV. $\eta\pi^+\pi^-$ ANALYSIS

The first event selection is equivalent to that used for the $K^+K^-\pi^0$ channel except for the pion-mass assumption for the charged tracks. The selected events are 2C fit by imposing the η mass to every photon pair. The combination giving the lowest χ^2 is retained and the events with $\chi^3 > 3$ are rejected.

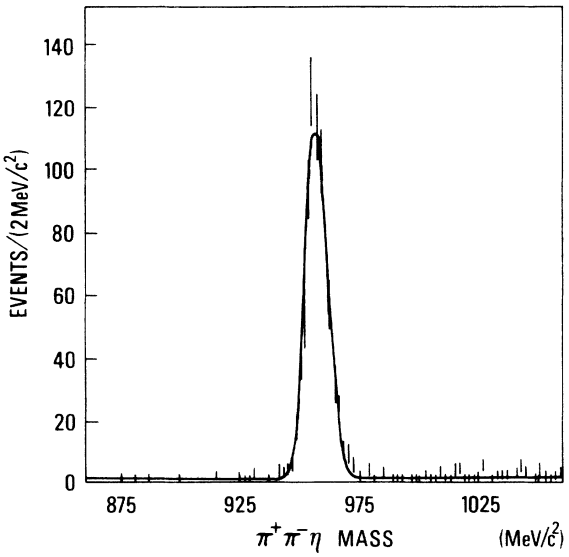

FIG. 9. $\eta' \to \eta\pi^+\pi^-$ signal for $J/\psi \to \gamma\pi^+\pi^-\eta$ events.

Figure 9 gives evidence of η' signal. From a fit to a Gaussian curve the η' mass value is obtained:

$$m_{\eta'} = 958.2 \pm 0.4 \text{ MeV}/c^2$$

with a mass resolution $\sigma_{\eta'} = 4.4 \pm 0.2$ MeV/c^2. From 622 η' events and an efficiency of $(11.5 \pm 0.5)\%$ the branching ratio is calculated:

$$B(J/\psi \to \gamma\eta') = (4.04 \pm 0.16 \pm 0.85) \times 10^{-3} \ .$$

Figure 10 shows the scatter plot $m_{\eta\pi}$ versus $m_{\eta\pi\pi}$ for the events with $1000 < m_{\eta\pi\pi} < 1800$ MeV/c^2. The $\eta\pi\pi$ mass distribution [Fig. 11(a)] gives evidence of two structures

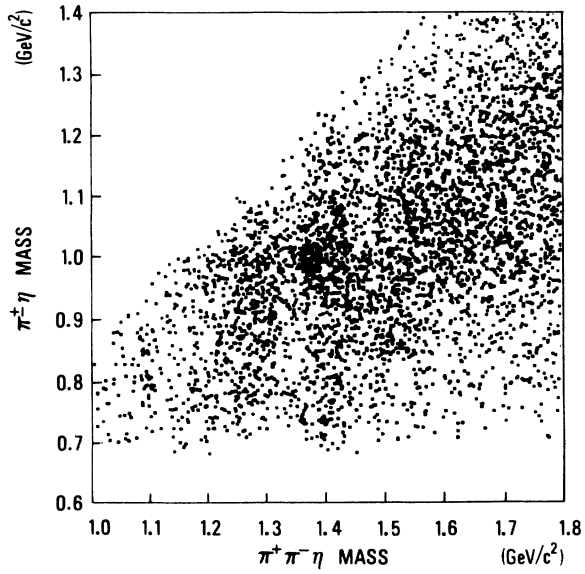

FIG. 10. $\eta\pi^\pm$ mass vs $\eta\pi^+\pi^-$ mass-scatter plot (two entries per event).

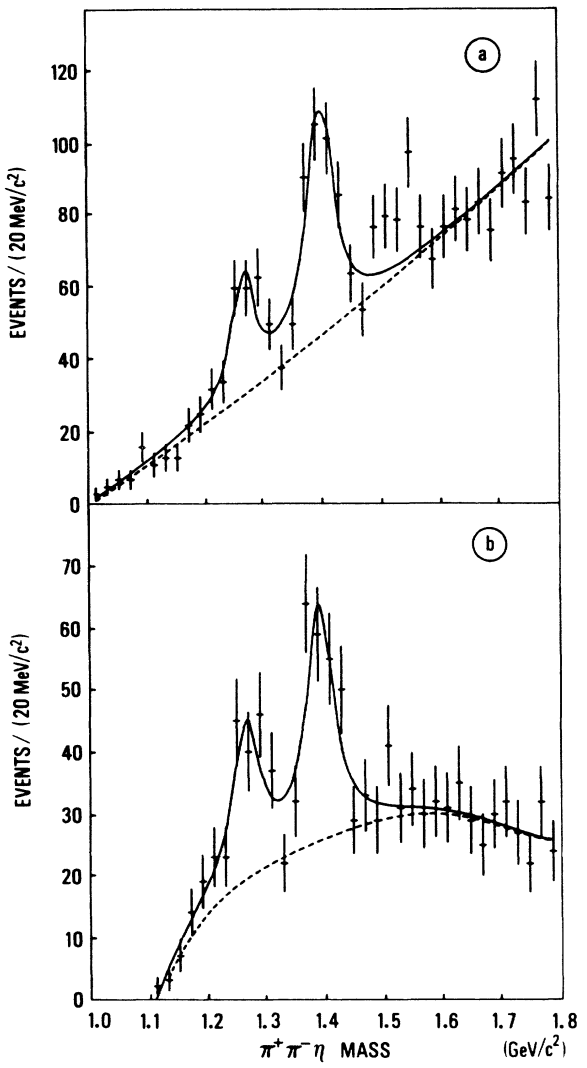

FIG. 11. Fit of the $\pi^+\pi^-\eta$ mass distribution in the 1–2-GeV/c^2 mass range for (a) $J/\psi\to\gamma\pi^+\pi^-\eta$ events before and (b) after the $a_0(980)\pi$ cut.

on a rising background, whereas no signal is observed at the $\eta(1430)$ mass. Many J/ψ decays contribute to the background in Fig. 10 ($J/\psi\to\gamma\eta$, $\omega\pi^0$, ρA_2, etc.). But a Monte Carlo study of these backgrounds shows that the overall behavior is smooth in the whole range of interest. So the two structures have been fit to two Breit-Wigner functions added to a polynomial background giving the parameters

$$m_1=1264\pm8\ \text{MeV}/c^2,\quad m_2=1398\pm6\ \text{MeV}/c^2,$$

$$\Gamma_1=44\pm20\ \text{MeV}/c^2,\quad \Gamma_2=53\pm11\ \text{MeV}/c^2.$$

The first peak can be associated to the $f_1(1285)$ or $\eta(1275)$. Signals at about the same mass have been reported by DM2 in radiative[18] and hadronic[15,19] J/ψ decays. Concerning the second peak a state has been observed at the same mass and in the same final state at KEK[20] in $\pi^-p\to n\pi^+\pi^-\eta$ reaction. From 108 ± 17 and 261 ± 24 events, respectively, the branching ratios are quoted:

$$B(J/\psi\to\gamma X(1264))B(X(1264)\to\eta\pi^+\pi^-)=(0.26\pm0.04\pm0.04)\times10^{-3},$$

$$B(J/\psi\to\gamma X(1398))B(X(1398)\to\eta\pi^+\pi^-)=(0.70\pm0.06\pm0.11)\times10^{-3}.$$

The projection [Fig. 12(a)] on the $m_{\eta\pi}$ axis of the scatter plot of Fig. 10 shows evidence of an important $a_0(980)$ dynamics ($m=988\pm2$, $\Gamma=48\pm3$ MeV/c^2). A cut on the $\eta\pi^\pm$ mass, $930\le m_{\eta\pi}\le1030$ MeV/c^2, is made in order to isolate events with such a dynamics. Figure 11(b) exhibits the two states previously observed. Their mass and width do not undergo noticeable variations. However the limited phase space available to the $\eta\pi$ system does not permit us to state if a real $a_0(980)$ dynamics is present in the $X(1264)$ decays [Fig. 12(b)]. A clean signal is on the contrary observed if the $X(1398)$ is considered [Fig. 12(c)]. Thus a branching ratio is calculated only for the latter and using an efficiency of $(8.2\pm0.5)\%$ the value is obtained

$$B(J/\psi\to\gamma X(1398))B(X(1398)\to a_0^\pm\pi^\mp)B(a_0^\pm\to\eta\pi^\pm)=(5.6\pm0.7\pm0.9)\times10^{-4}.$$

A further enhancement around 1545 MeV/c^2, $\simeq40$ MeV/c^2 wide, may be present in the $\eta\pi^+\pi^-$ mass distribution of Fig. 11(a). This signal is depressed if the $a_0(980)\pi$ cut is applied. It is noticeable that a state has been observed at the same mass by the LASS experiment[21] in the $K\bar{K}\pi$ final state.

Finally by requiring the $a_0(980)\pi$ dynamics no $\eta(1430)$ signal appears. We recall that the $\eta(1430)$ is expected to

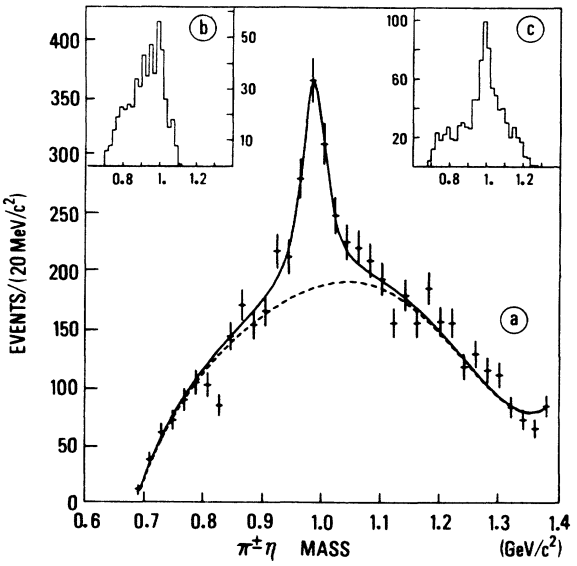

FIG. 12. (a) $\eta\pi$ mass distribution for the $J/\psi\to\gamma\eta\pi^+\pi^-$ events, (b) for the events into the $X(1264)$, and (c) the $X(1398)$ window.

decay into $\eta\pi\pi$ if the $K\bar{K}\pi$ mode goes through an $a_0(980)\pi$ intermediate state. A maximum $\eta(1430)$ contribution has been evaluated by assuming the $X(1398)$ as a sum of two separate signals one of which is the $\eta(1430)$. By fitting the mass distribution of Fig. 11(b) to three Breit-Wigner functions, two of them fixed to the $X(1264)$ and $\eta(1430)$ parameters, added to a polynomial background, the number of $\eta(1430)\to\eta\pi^+\pi^-$ decays is evaluated to be at most 50 events and leads to the upper limit, at 90% C.L.,

$$B(J/\psi\to\gamma\eta(1430))B(\eta(1430)\to a_0^{\pm}\pi^{\mp})B(a_0^{\pm}\to\eta\pi^{\pm}) < 1.8\times10^{-4} .$$

From this result the ratio is inferred

$$\frac{B(\eta(1430)\to a_0(980)\pi\to\eta\pi\pi)}{B(\eta(1430)\to K\bar{K}\pi)} < 7.5\% .$$

This limit is incompatible with a supposed dominant $a_0(980)\pi$ dynamics in the $\eta(1430)\to K\bar{K}\pi$ decay. The $\eta\pi\pi$ suppression has been interpreted[22] in terms of a $K\bar{K}$ molecule nature of the $f_0(975)$ and $a_0(980)$. On the other hand, it has been proposed[23] that a 0^- glueball with a mass around 1450 MeV/c^2 would mainly decay into $K\bar{K}\pi$ with an important $KK^*(892)$ contribution.

V. $\rho\gamma$ ANALYSIS

The sample of events with two oppositely charged tracks and two isolated photons in the barrel detector are 2C fit to the kinematical hypothesis $J/\psi\to\pi^+\pi^-\gamma\gamma$.

The $\pi\pi\gamma\gamma$ candidates are further selected by a cut on the squared missing mass ($<0.6\times10^6$ MeV$^2/c^4$) of the system recoiling against the $\pi^+\pi^-$ system in order to eliminate events from $\pi^+\pi^-\pi^0$, $\pi^+\pi^-\eta$, and $\omega\pi^0$ channels. A visual scan of the events for which the lowest $\pi^+\pi^-\gamma$ mass is greater than 1050 MeV/c^2 shows that two categories of background are still present.

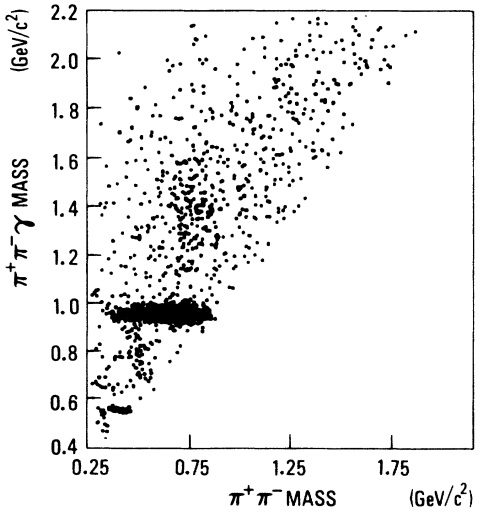

FIG. 13. $\pi^+\pi^-\gamma$ mass vs $\pi^+\pi^-$ mass-scatter plot for $J/\psi\to\gamma(\pi^+\pi^-\gamma)$ events.

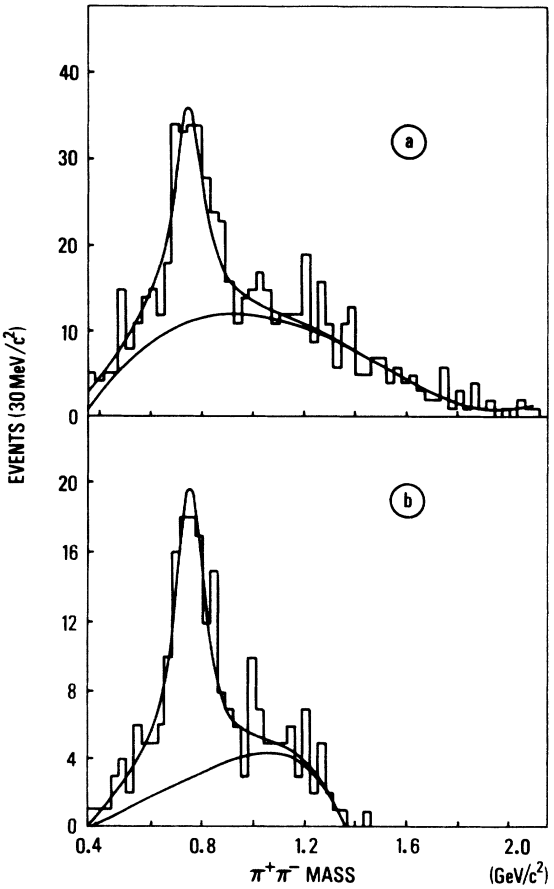

FIG. 14. $\pi^+\pi^-$ mass for $J/\psi\to\gamma\rho\gamma$ events (a) with $m_{\pi^+\pi^-\gamma}>1.05$ GeV/c^2 and (b) with $1.3<m_{\pi^+\pi^-\gamma}<1.6$ GeV/c^2.

(i) Events with one misidentified photon which can be attributed to the channel $J/\psi\to\gamma K_L^0 K^{\pm}\pi^{\mp}$. The track found in the photon detector has no shower signature and is typical of a K_L^0 interaction.

(ii) Events with higher π^0 multiplicity which are evidenced by isolated tracks in the end-cap detector and/or

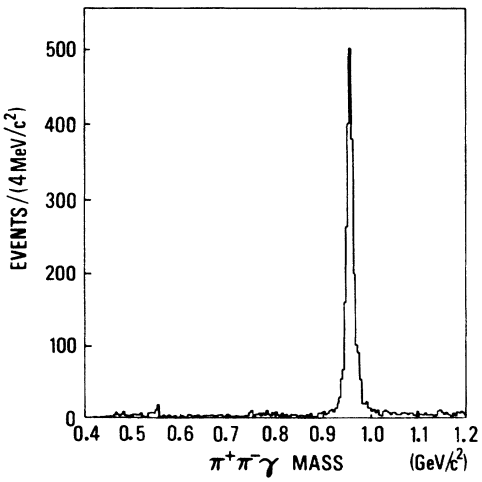

FIG. 15. $\eta'\to\rho\gamma$ signal for $J/\psi\to\gamma\rho\gamma$ events.

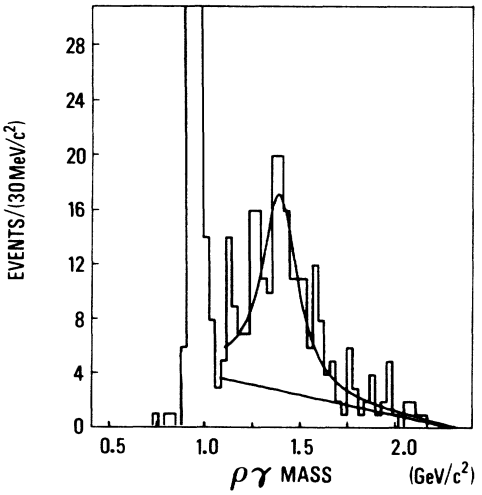

FIG. 16. $\rho\gamma$ invariant-mass distribution for $J/\psi\to\gamma\rho\gamma$ events in the $\eta(1430)$ mass region.

significant extra energy in the scintillators often associated to a few hits which have not been recognized as a photon by the barrel-tracking routine.

Then two other cuts are applied: A time-of-flight cut requires at least one track to be consistent, within 2.5σ, to a pion-mass assignment and no isolated track must be found in the photon end-cap detector. To further reduce higher π^0 multiplicity events a pattern cut associating scintillator amplitudes and tube hits in the barrel detector is used. This cut has been tested on the clean $\eta'\gamma$ signal to produce a 1% loss of events while it removes 12% of the low-$\pi\pi\gamma$-mass events above the η'.

Direct indication of a $\rho\gamma$ signal around 1400 MeV/c^2 can be seen in Fig. 13 where, for the lowest $\pi^+\pi^-\gamma$ mass combination, the $\pi^+\pi^-$ mass against the $\pi^+\pi^-\gamma$ mass is plotted. Evidence for a ρ signal is shown in Figs. 14(a) and 14(b). The amount of no-ρ events is estimated by fitting these distributions to a Breit-Wigner curve added to a quadratic function. Defining a ρ cut by $625 \le m_{\pi^+\pi^-} \le 925$ MeV/c^2, the ratio $R=(\rho$ events$)$ / (no-ρ events) is 1.20 ± 0.05 for $m_{\pi^+\pi^-\gamma} > 1050$ MeV/c^2 [Fig. 14(a)] and rises up to 3.0 ± 0.5 for $1300 \le m_{\pi^+\pi^-\gamma} \le 1600$ MeV/c^2 [Fig. 14(b)].

Figure 15 shows the $\pi^+\pi^-\gamma$ mass distribution after cutting on the ρ mass. A fit of the η' peak to a Gaussian curve gives the η' mass value

$$m_{\eta'}=957.8\pm0.2 \text{ MeV}/c^2 .$$

The experimental resolution is $\sigma_{\eta'}=7.9\pm0.2$ MeV/c^2. The 2420η' events correspond to the branching ratio

$$B(J/\psi\to\gamma\eta')=(4.39\pm0.09\pm0.66)\times10^{-3}$$

in agreement with the value obtained in the $\eta\pi\pi$ decay mode.

In addition to the large η' signal there are events accumulating in the $\eta(1430)$ mass region (Fig. 16). The distribution can be fitted to a single Breit-Wigner curve added to a linearly falling background determined from the events discarded by the last three cuts. One obtains

$$m_X=1401\pm18 \text{ MeV}/c^2, \quad \Gamma_X=174\pm44 \text{ MeV}/c^2 ,$$

$$R=1.15\pm0.16 .$$

The value of R is close to the estimate made in Fig. 14(a). For 123 ± 20 events and an efficiency equal to $(15.0\pm0.2)\%$ one can calculate the branching ratio

$$B(J/\psi\to\gamma X(1401))B(X(1401)\to\rho^0\gamma) = (0.95\pm0.20\pm0.14)\times10^{-4} .$$

The obtained parameters are consistent with other previously reported measurements in the same channel.[24] Nevertheless width and mass are poorly consistent with the values found for the $\eta(1430)$ in the $K\bar{K}\pi$ decay. Therefore it seems difficult to identify the observed signal with the $\eta(1430)$. The low statistics does not permit to conclude if more states contribute. However two structures might be present around 1300 and 1400 MeV/c^2 as observed in the $\eta\pi^+\pi^-$ channel. New results from the Mark III experiment[25] give evidence of two states.

VI. SUMMARY

The $\eta(1430)$ signal is observed in the $J/\psi\to\gamma K^+K^-\pi^0$ and $J/\psi\to\gamma K_S^0K^\pm\pi^\mp$ decays and a high-statistics measurement of its parameters is performed. Some $\eta(1430)$ properties can be summarized.

(a) A three-body decay-angular analysis privileges a $J^P=0^-$ assignment.

(b) A Dalitz-plot analysis shows an important $KK^*(892)$ dynamics.

(c) The shape of the low-$K\bar{K}$-mass distribution is compatible with the presence of an $a_0(980)\pi$ intermediate state, but no clear evidence of this dynamics is found within this analysis.

(d) No $\eta(1430)$ signal is observed in the $J/\psi\to\gamma\eta\pi^+\pi^-$ mode, even if the $a_0(980)\pi$ dynamics is required.

The problem of a possible compositeness of the $\eta(1430)$ signal is not answered by the present study. A full wave analysis in progress deals with it.

Furthermore the analysis of the $J/\psi\to\gamma\eta\pi^+\pi^-$ decay shows in the $\eta\pi\pi$ mass spectrum a peak in the $f_1(1285)/\eta(1275)$ mass range and a new state at 1398 MeV/c^2, $\simeq50$ MeV/c^2 wide. At least the last state is compatible with a large-$a_0(980)^\pm\pi^\mp$ dynamics. Their spin-parity assignment will be discussed in a forthcoming paper. Moreover a further new state might be present around 1550 MeV/c^2.

The signal observed in the low-statistics $J/\psi\to\gamma\rho\gamma$ decay measurement is hardly consistent with the $\eta(1430)$. The $\rho^0\gamma$ mass spectrum might be compatible with that observed in the $\eta\pi\pi$ mode.

[1]H. Fritzsch and M. Gell-Mann, in *Proceedings of the XVI International Conference on High Energy Physics,* Batavia, Illinois, 1972, edited by J. D. Jackson and A. Roberts (NAL, Batavia, IL, 1973); G. Bhanot, Phys. Lett. **101B**, 95 (1981); J. F. Donoghue *et al.*, *ibid.* **99B**, 416 (1981); J. Coyne *et al.*, *ibid.* **91B**, 259 (1980).

[2]D. Scharre *et al.*, Phys. Lett. **97B**, 329 (1980).

[3]C. Edwards *et al.*, Phys. Rev. Lett. **49**, 259 (1982).

[4]S. Blessing, in *Intersections Between Particle and Nuclear Physics,* proceedings of 3rd Conference, Rockport, Maine, 1988, edited by G. Bunce (AIP Conf. Proc. No. 176) (AIP, New York, 1988).

[5]D. P. Stanley and D. Robson, Phys. Rev. D **21**, 3180 (1980); S. Goffrey and N. Isgur, *ibid.* **32**, 189 (1985).

[6]P. Baillon *et al.*, Nuovo Cimento **50A**, 393 (1967); C. Dionisi *et al.*, Nucl. Phys. **B169**, 1 (1980); T. A. Armstrong *et al.*, Phys. Lett. **146B**, 273 (1984).

[7]D. O. Caldwell, Mod. Phys. Lett. A **2**, 771 (1987).

[8]A. Birman *et al.*, Phys. Rev. Lett. **61**, 1557 (1988); T. A. Armstrong *et al.*, Phys. Lett. B **221**, 216 (1989); N. G. Rath *et al.*, Phys. Rev. D **40**, 693 (1989).

[9]A. Ando *et al.*, Phys. Rev. Lett. **57**, 1296 (1986).

[10]K. Senba and M. Tanimoto, Lett. Nuovo Cimento **35**, 295 (1982); T. Barnes and F. E. Close, Report No. RAL 84-055, 1984 (unpublished); J. Donoghue, Phys. Rev. D **30**, 114 (1984).

[11]W. F. Palmer and S. Pinsky, Phys. Rev. D **27**, 2219 (1983); W. F. Palmer, S. Pinsky, and C. Bender, *ibid.* **30**, 1002 (1984).

[12]J. E. Augustin *et al.*, Phys. Scr. **23**, 623 (1981).

[13]This analysis is relative to 7.1×10^6 J/ψ's.

[14]The possibility that more than one state contributes to the observed $\eta(1430)$ signal is not checked in this paper.

[15]J. Jousset *et al.*, Phys. Rev. D **41**, 1389 (1990).

[16]M. Jacob and G. Wick, Ann. Phys. (N.Y.) **7**, 404 (1959); S. Berman and M. Jacob, Phys. Rev. **139**, B1023 (1965).

[17]S. Flatté, Phys. Lett. **63B**, 224 (1976).

[18]D. Bisello *et al.*, Phys. Rev. D **39**, 701 (1989).

[19]A. Falvard *et al.*, Phys. Rev. D **38**, 2706 (1988).

[20]S. Fukui *et al.*, *Hadron '87,* in proceedings of the 2nd International Conference on Hadron Spectroscopy, Tsukuba, Japan, 1987, edited by Y. Oyanagi, K. Takamatsu, and T. Tsuro (KEK Report No. 87-7, Tsukuba, 1987).

[21]B. Ratcliff, in *Glueballs, Hybrids, and Exotic Hadrons,* proceedings of BNL Workshop, Upton, New York, 1988, edited by S.-U. Chung (AIP Conf. Proc. No. 185) (AIP, New York, 1989).

[22]M. Frank *et al.*, Phys. Rev. D **32**, 2971 (1985).

[23]G. J. Gounaris and H. Neufield, Phys. Lett. B **213**, 541 (1988).

[24]D. Hitlin, in *Proceedings of 1983 International Symposium on Lepton and Photon Interactions at Hight Energies,* Ithaca, New York, 1983, edited by D. G. Cassel and D. L. Kreinick (Newman Laboratory of Nuclear Studies, Cornell University, Ithaca, 1983).

[25]D. Coffman *et al.*, Report No. SLAC-PUB-5104, 1989 (unpublished).